Hydroelectric Regulation Decouples Arctic Silica Delivery from the Diatom Bloom: A Climate-Independent Causal Attribution Across Twenty Subarctic Rivers

Ali Bin Shahid

PSKL Water for All, Islamabad, Pakistan

ORCID: 0009-0003-9709-4241

Correspondence:ali@paanisubkayliay.com

Preprint disclosure. This is a non-peer reviewed preprint submitted to EarthArXiv. The manuscript has not yet been submitted to a journal for peer review at the time of posting. Subsequent versions may differ from this version.

Data and code availability. Analysis code and derived data are available at github.com/R3GENESI5/subarctic-dam-nutrient-timing-analysis, archived on Zenodo with concept DOI 10.5281/zenodo.20356090 (v1.0.0 version DOI 10.5281/zenodo.20356091). The primary data are the Arctic Great Rivers Observatory (ArcticGRO) water-quality and discharge datasets and the Global Aggregation of Stream Silica dataset (Jankowski et al., 2025).

AI disclosure. Portions of this manuscript were drafted and edited with AI language model assistance. All scientific analysis, interpretation, data verification, and responsibility for claims rest with the author.

Abstract

Large subarctic rivers deliver most of their dissolved nutrients during the spring freshet, in approximate phase with the ice-edge diatom bloom that those nutrients support. Hydroelectric regulation flattens the river hydrograph, holding back the freshet and raising winter discharge, and in doing so it redistributes nutrient delivery in time. Across twenty subarctic rivers spanning the Arctic Ocean and Bothnian Bay drainages, classified by basin-cumulative Degree of Regulation (DOR), we test whether regulation shifts the delivery of dissolved silica out of phase with the shelf-specific diatom bloom window. Using the Global Aggregation of Stream Silica dataset (Jankowski et al., 2025) and the Arctic Great Rivers Observatory record, we estimate seasonal silica flux with a LOADEST-style concentration-discharge rating and map delivery onto receiving-shelf bloom climatology for eight shelves (Kara, Laptev, East Siberian, Beaufort, Bering/Chukchi, Bothnian Bay, Bothnian Sea, Gulf of Finland). Regulated rivers deliver 24.8 percent of annual silica during the open-water bloom window against 35.8 percent for controls, a synchrony gap of -11.0 percentage points that remains negative under every combination of plus-or-minus 15-day perturbations of the bloom window (49 of 49 negative, range -7.3 to -13.8 pp). The synchrony loss scales monotonically with DOR across the panel (Spearman rho = -0.80; OLS slope -0.284 per unit DOR, R-squared = 0.59, t = -5.05, two-sided p = 0.00008 from Student-t with n = 20 rivers spanning DOR 0 to 0.63), and leave-one-out cross-validation preserves a negative slope in 20 of 20 fits (slope range -0.310 to -0.250, all p less than 0.001). A placebo difference-in-differences design argues against the climate-only counterfactual on the cleanest available natural experiment: post-Krasnoyarsk Yenisei shifted winter discharge fraction by 4.96 percentage points more than the unregulated Lena (95 percent CI 4.21 to 5.72, p less than 0.0001) under identical Siberian climate. Within Yenisei, the year-by-year differential winter discharge fraction tracks the cumulative basin reservoir-filling curve across 73 years (r = +0.82), converting the binary causal test into a continuous-dose trajectory. The expanded twenty-river panel reproduces the original six-river ArcticGRO result independently (gap -10.0 vs -9.2 pp on the same six rivers using GlASS data), with multiple high-DOR anchors (Yenisei, Lulealven, Indalsalven, Skellefte, Oulujoki, Kymijoki, Angermanalven) replacing the single-river leverage of the original analysis. The contribution is the reframing of regulated-river nutrient alteration from a winter-enhancement story to a measurable loss of synchrony between SiO2 delivery and biological demand on the receiving shelves, robust across the Arctic Ocean and Bothnian Bay drainages.

---

1. Introduction

1.1 Subarctic rivers, the freshet, and nutrient delivery

The large rivers draining the pan-Arctic watershed deliver freshwater, dissolved nutrients, and organic matter to the seasonally ice-covered shelf seas that ring the Arctic Ocean. In their unregulated state these rivers are strongly pulsed. Snowmelt produces a freshet in late spring and early summer that carries the majority of the annual water volume and a correspondingly large share of the annual nutrient load (Holmes et al., 2012). This pulse is approximately in phase with the return of light and the retreat of sea ice, and therefore with the spring phytoplankton bloom that the delivered nutrients support.

The timing of nutrient delivery, not only its magnitude, is biologically consequential. A nutrient delivered to a sunlit, ice-free, biologically active surface layer is available to primary producers; the same nutrient delivered beneath winter sea ice, into a dark and deeply mixed water column, is not. Whether it remains available months later, when the bloom finally begins, depends on advection and vertical mixing during the intervening ice-covered period.

1.2 Hydroelectric regulation alters the hydrograph

Hydroelectric regulation reshapes the seasonal distribution of river discharge. A reservoir stores a portion of the spring and summer inflow and releases it through the following autumn and winter to meet year-round electricity demand. The characteristic signature is a flattened hydrograph: a reduced summer maximum and an elevated winter minimum (Humborg et al., 2006). Because dissolved constituents are transported by the water, regulation that moves water from summer into winter also moves the constituents the water carries.

This hydrological redistribution has been documented at the basin scale. Humborg et al. (2006) compared the regulated Lule River with the adjacent pristine Kalix River in northern Sweden and found the winter fraction of transported silica, organic carbon, iron, and phosphorus to be two to three times higher in the regulated river. Maavara et al. (2020) review the broader evidence that river damming alters the biogeochemical cycling of carbon, nitrogen, phosphorus, and silicon. Guzzi et al. (2024) reported that hydroelectric development of the La Grande River in James Bay shifted peak freshwater discharge from spring into winter and altered the seasonality of nitrate and phosphate in the receiving coastal zone.

1.3 Silica and the diatom bloom

Among the nutrients a river carries, dissolved silica occupies a distinct position. Silica is the obligate building material of the diatom frustule. Diatoms cannot substitute another element for it, and diatom growth in many systems is silica-limited. In the seasonally ice-covered seas of the Arctic and subarctic, the spring bloom is diatom-dominated, and the silica-demanding fraction of the phytoplankton community appears predominantly during the under-ice and ice-edge bloom period (Arrigo et al., 2012; and references in Section 3.4).

The Arctic spring bloom is sharply time-compressed relative to temperate systems. It is gated by the return of light and the retreat of sea ice, and it tracks the ice edge as a pulse lasting weeks rather than months. Sea-ice break-up on the major Siberian and Beaufort shelves occurs in mid to late June (Stroeve et al., 2014). The window during which delivered silica can be drawn down by a diatom bloom is therefore narrow and seasonally fixed.

The strategic consequence of damming has a precedent in the temperate literature. Humborg et al. (1997) showed that silica retention behind Danube River dams reduced silica delivery to the Black Sea, contributing to a shift in the phytoplankton community away from diatoms. That work concerned a change in the silica budget. The question we address concerns a change in the silica schedule.

1.4 The gap and this study

Two limitations of the existing literature motivate this study. First, the documented cases are single systems: the Lule in Sweden, the La Grande in Canada. No study has compared the seasonal nutrient signature of regulation across the pan-Arctic river system in a single consistent analysis. Second, the regulation signal has not been cleanly separated from the background climate trend. Lee et al. (2023), synthesizing nutrient inputs to Hudson Bay, identified the attribution of seasonal change to regulation versus climate as an open problem.

We address both. We assemble a six-river comparison spanning Siberia and northern North America, we separate regulation from climate by pairing regulated rivers against minimally regulated controls subject to the same regional climate forcing, and we ask a specific question of the silica record: does regulation shift silica delivery out of phase with the diatom bloom that silica supports?

---

2. Data and Methods

2.1 Rivers and regulation status

We analyze twenty subarctic rivers across two ocean drainages. **Six Arctic Ocean rivers** monitored by the Arctic Great Rivers Observatory (ArcticGRO): the Ob, Yenisei, Lena, and Kolyma in Siberia, and the Mackenzie and Yukon in northern North America – these are the foundational panel and the only basin within which we run the long-record discharge-shift test (Section 3.1) and the within-river storage-tracking analysis (Section 3.10) because their daily discharge records extend to 1936. **Fourteen additional Bothnian Bay, Bothnian Sea, and Gulf of Finland rivers** from the Global Aggregation of Stream Silica dataset (Jankowski et al., 2025): Lulealven, Kalixalven, Pite, Skellefte, Tornio (Finnish gauge), Iijoki, Kemijoki, Oulujoki (Bothnian Bay); Angermanalven, Indalsalven, Ume, Dalalven, Ljusnan (Bothnian Sea); Kymijoki (Gulf of Finland). These extend the cross-sectional dose-response (Sections 3.6 to 3.9) to multiple high-DOR anchors and four times the bloom-window-sample density.

The expanded panel is classified by basin-cumulative Degree of Regulation (DOR; Section 2.7). For descriptive comparisons we use an a priori binary status (regulated when DOR $>= 0.14$, control when DOR < 0.10) but the headline analyses treat DOR as a continuous predictor.

- **Regulated (14 rivers):** Yenisei (DOR 0.63), Lulealven (0.55), Skellefte (0.46), Indalsalven (0.43), Oulujoki (0.40), Ljusnan (0.40), Kymijoki (0.38), Angermanalven (0.34), Dalalven (0.31), Ume (0.28), Mackenzie (0.26), Kemijoki (0.20), Iijoki (0.17), Ob (0.15).
- **Control (6 rivers):** Kolyma (DOR 0.14, mid-range but lower-river permafrost-overrides upstream regulation), Pite (0.09), Lena (0.07), Yukon (0.002), Kalixalven (0.000), Tornio (0.000). Lena carries the Vilyuy reservoir on a tributary; we retain it as the unregulated placebo for the Yenisei discharge-shift test because its main-stem hydrograph at the mouth is close to natural.

The paired and continuous designs together separate regulation from climate. The binary contrast (Sections 3.2 and 3.6) gives a clean before-after-control-after style comparison; the DOR continuum (Section 3.8) treats regulation as a quantitative dose-response across the panel; and the Yenisei-Lena natural experiment (Sections 3.1 and 3.10) provides the within-river causal anchor.

2.2 Data sources

Water-quality concentrations for dissolved nitrate (NO3), ammonium (NH4), total dissolved nitrogen (TDN), dissolved silica (SiO2), and dissolved organic carbon (DOC) for the six Arctic rivers are from the ArcticGRO water-quality dataset, covering 2003 to 2024. The record consists of grab samples, with between 83 and 103 valid samples per river and parameter, of which 16 to 30 fall in the winter season. Daily discharge for the six rivers, 1936 to 2025, is from the ArcticGRO discharge dataset, which compiles gauge records from Roshydromet (Eurasian rivers), the Water Survey of Canada (Mackenzie), and the United States Geological Survey (Yukon).

Dissolved silica concentrations and daily discharge for the fourteen Bothnian Bay, Bothnian Sea, and Gulf of Finland rivers are from version 2.0 of the Global Aggregation of Stream Silica (GlASS) dataset (Jankowski et al., 2025), which compiles measurements from national monitoring networks worldwide. For Swedish rivers GlASS draws from the SMHI environmental monitoring programme; for Finnish rivers from the Finnish Environmental Institute (SYKE) hydrochemistry archive. Coverage spans 2000-2023 for most rivers, with 50-156 winter SiO2 samples per river – three to seven times the ArcticGRO winter sample density per river. Values reported as below detection were excluded from the rating fit. We additionally cross-validate the six ArcticGRO rivers against their independent GlASS-incorporated chemistry; the two datasets agree to within roughly one percentage point on the in-bloom silica fraction per river.

2.3 Seasonal definitions and the discharge shift test

Seasons are defined as winter (December to March), spring (April to June), summer (July to September), and fall (October to November). For the long discharge record we compute, per river and water year, the fraction of annual discharge volume delivered in winter, and compare the pre-regulation era (water years before 1967) with the post-regulation era (after 1978) for the Yenisei against the Lena control.

2.4 Seasonal silica flux: a concentration-discharge rating

Estimating a seasonal load from sparse grab samples and a continuous discharge record requires care, because concentration and discharge covary. We use a concentration-discharge (C-Q) rating in the form established for the USGS LOADEST framework (Runkel et al., 2004). For each river and parameter we fit, on the paired sample concentration and same-day discharge:

$\ln(C) = b0 + b1\ z + b2\ z^2 + b3 \sin(2\ pi\ d) + b4 \cos(2\ pi\ d) + b5\ t$

where C is concentration, z is the centered natural logarithm of discharge, d is the day of year expressed as a fraction, and t is centered decimal time. The fitted rating is applied to every day of the daily discharge record within the sampled span to predict daily concentration. Retransformation bias from the logarithmic fit is removed with the Duan (1983) smearing estimator. Daily load is the product of predicted concentration and daily discharge, and seasonal load fractions follow by summation.

2.5 Four-way reconciliation of the flux estimate

Because the choice of flux estimator can itself influence the result, we estimate the winter load fraction four ways and report the spread:

- **A, mean concentration:** seasonal mean concentration multiplied by seasonal discharge volume.
- **B, flow-weighted:** seasonal flow-weighted mean concentration multiplied by seasonal discharge volume.
- **C, rating, quadratic:** the six-term C-Q rating of Section 2.4.
- **D, rating, linear:** the rating with the z^2 term removed.

Methods A and B use observed concentrations only and involve no curve extrapolation; C and D are rating curves. A parameter for which all four methods agree is treated as robust; a parameter for which they diverge is treated as method-sensitive and is not used for headline inference.

2.6 The decoupling metric

To express the biological relevance of delivery timing we map the silica delivery schedule onto the diatom bloom window. The bloom window is taken from the published sea-ice and bloom-phenology literature (Section 3.4): under-ice diatom blooms can begin at approximately the start of May, and open-water blooms follow sea-ice break-up, which occurs on a shelf-specific date in mid to late June for the Siberian and Beaufort shelves. We report two thresholds for the fraction of annual silica delivered before the bloom can use it: a pre-May fraction (delivered December to April, while the shelf is ice-covered and dark) and a pre-break-up fraction (delivered before the receiving shelf opens).

2.7 Basin-cumulative Degree of Regulation

We quantify regulation continuously rather than as a binary status. Degree of Regulation (DOR) follows the convention of Nilsson et al. (2005) and Grill et al. (2019): basin-cumulative upstream reservoir storage capacity divided by mean annual discharge at the river-mouth gauge, dimensionless. We use the GRanD reservoir database (Lehner et al., 2011) cross-checked against ICOLD entries for cited storage capacities, and mean annual discharge computed directly from the ArcticGRO daily record. Basin-cumulative storage sums all reservoirs upstream of the mouth gauge, including those on major tributaries, because the regulated flow propagates to the mouth.

Computed DOR values: Yenisei 0.63 (Krasnoyarsk 73.3 + Sayano-Shushenskoye 31.0 main stem; Angara cascade 287.4 – Irkutsk 2.1, Bratsk 168.2, Ust-Ilimsk 58.9, Boguchany 58.2), Mackenzie 0.26 (W.A.C. Bennett 74.0 on Peace tributary), Ob 0.15 (Novosibirsk 8.8 main stem; Bukhtarma 50.0 on Irtysh), Kolyma 0.14 (Kolymskaya 15.1), Lena 0.07 (Vilyuy 35.9 on Vilyuy tributary), Yukon 0.002 (Whitehorse Rapids, negligible).

The binary regulated/control classification used in Section 2.1 is retained for compatibility with the discharge-shift test (Section 2.3) and the silica panel (Section 3.2), but the dose-response analyses in Sections 3.7 to 3.9 use DOR as a continuous predictor.

2.8 Robustness, dose-response, and time-resolved designs

Four additional analyses extend the binary regulated-versus-control comparison.

Bloom-window sensitivity sweep. Because the synchrony metric depends on the chosen bloom window, we perturb the (start_DOY, end_DOY) per shelf by Delta_start in {-15, -10, -5, 0, +5, +10, +15} days and Delta_end by the same set, recomputing the regulated-minus-control synchrony gap at all 49 combinations.

DOR dose-response regression. For each river we regress the in-bloom silica fraction on basin-cumulative DOR by ordinary least squares and report Spearman rho as a rank-correlation alternative more honest at n = 6.

Joint DOR-by-window sensitivity. We combine the two sensitivity dimensions by recomputing the DOR regression at each of the 49 bloom-window perturbations, reporting the slope, R-squared, and Spearman rho on the perturbation grid.

Bootstrap difference-in-differences (DiD). The discharge-shift test of Section 2.3 is extended with a

block-bootstrap confidence interval: 5000 iterations of resampling within each (river by pre/post) cell. Single water-year blocks are the primary specification. The annual winter Q fraction time series carries non-trivial autocorrelation that we report explicitly per river (lag-1 rho: Yenisei +0.83, Lena +0.57, Kolyma +0.55, Yukon +0.45, Ob +0.37, Mackenzie -0.19). A 5-year moving-block sensitivity check yields confidence intervals approximately 18-33% wider than the single-year-block intervals (Yenisei-Lena DiD: CI widens from +/- 0.79 pp to +/- 1.05 pp around the point estimate; Ob-Lena DiD: CI widens from +/- 0.93 pp to +/- 1.10 pp). The Yenisei-Lena DiD remains overwhelmingly significant under both block specifications ($p < 0.0001$); the Ob-Lena DiD remains non-significant under both. The one-sided p-value is computed from the bootstrap distribution of (Delta_regulated - Delta_control).

Storage-filling time-resolved trajectory. For each regulated river we reconstruct the cumulative basin-storage curve from commissioning dates and capacities of all upstream reservoirs, and compute the year-by-year winter discharge fraction. We then correlate (Pearson r) the storage curve against (i) the raw winter fraction and (ii) the climate-corrected differential winter fraction (regulated minus paired unregulated control).

All analysis code and derived data are in the repository named in the Data Availability statement.

---

3. Results

3.1 Regulation has shifted discharge into winter

The long discharge record shows the expected hydrograph flattening on the regulated river and not on the control. The winter fraction of annual discharge on the Yenisei rose from 8.4 percent before 1967 to 15.2 percent after 1978. On the unregulated Lena, the same comparison gives 4.3 percent rising to 6.2 percent (Table 1). The Lena change of 1.9 percentage points is the regional climate-driven baseline; the Yenisei change of 6.8 points exceeds it by 4.9 points, a regulation-driven excess 3.5 times the size of the natural trend. A 5000-iteration block-bootstrap places the regulation-driven excess at +4.96 pp (95 percent CI [+4.21, +5.72]; one-sided $p < 0.0001$ against the climate-only null) when computed on water-year DJFM-over-annual ratios rather than on simple pre-period and post-period means, confirming the magnitude under a fully resampled null. An equivalent test for the Ob (Novosibirsk 1957 breakpoint) yields DiD = +0.68 pp (95 percent CI [-0.28, +1.57]), consistent with Novosibirsk being a single small dam relative to Ob's mean annual flow.

Table 1. Winter (December to March) fraction of annual discharge, regulated Yenisei versus control Lena.

River	Pre-1967	Post-1978	Shift
Yenisei (regulated)	8.4%	15.2%	+6.8 pp
Lena (control)	4.3%	6.2%	+1.9 pp
Regulation-driven excess			+4.9 pp

3.2 The six-river seasonal silica panel

Seasonal silica flux fractions, estimated by the C-Q rating, separate by regulation status (Table 2). The three regulated rivers deliver the largest winter fractions: Ob 26 percent, Yenisei 20 percent, Mackenzie 16 percent. The three controls deliver the smallest: Yukon 14 percent, Lena 10 percent, Kolyma 6 percent. Every river labeled regulated in Section 2.1 exceeds Lena and Yukon (the two lowest-DOR rivers); Kolyma sits between the unambiguous regulated and control sets, consistent with its intermediate DOR of 0.14 and the per-river residual analysis in Section 3.8. The Yukon is the highest of the unambiguous controls and approaches the Mackenzie, a point returned to in the Discussion.

3.3 The result is robust to the flux estimation method

The four-way reconciliation (Section 2.5) shows that the silica result does not depend on the estimator. For SiO2, and likewise for total dissolved nitrogen and dissolved organic carbon, the winter load fraction from the four methods agrees to within approximately one percentage point for every river (Table 2). The quadratic and linear ratings give nearly identical silica fractions, indicating that the result is not an artifact of curve shape.

Dissolved nitrate and ammonium behave differently. Their winter fractions vary by 15 to 30 percentage points across the four methods. This is a consequence of solute chemistry rather than of a flawed analysis: nitrate exhibits a strong inverse concentration-discharge relationship, being concentrated in low winter baseflow and diluted by the freshet, so its load estimate is acutely sensitive to how the freshet concentration minimum is treated. Ammonium ratings, in addition, are weak fits. We therefore do not use NO3 or NH4 as headline metrics, and base the inference on the three method-robust solutes. Silica is, in addition, the solute with the most direct biological interpretation.

A referee may reasonably ask how tightly the winter silica concentration itself is constrained, given the sparse winter sampling. Bootstrapping the winter SiO2 concentration per river (1000 iterations, resampling with replacement of the 17 to 30 winter samples per river) yields 95% confidence intervals whose width as a fraction of the winter mean ranges from 5.9% (Mackenzie) to 21.9% (Yukon), with a mean of 11.7% across the six rivers. The seasonal C-Q rating reduces this uncertainty further by borrowing strength from the full sample (including non-winter observations) through the seasonal terms in the fit; the winter load fractions in Table 2 are therefore point estimates whose underlying winter concentrations are constrained to within roughly +/- 5 to +/- 10% of the mean for most rivers and +/- 10 to +/- 15% for Yukon and Ob.

3.3a Stationarity of the C-Q rating

The LOADEST rating is fit on the full 2003-2024 sample pool and projected onto the full discharge record. If the silica concentration-discharge relationship has drifted within the sample period – as predicted by the reservoir-Si retention literature, where biogenic silica stripping by reservoir diatom blooms is strongest in young reservoirs and weakens over decades as buried silica accumulates (Conley et al., 2000; Humborg et al., 2006; Maavara et al., 2014) – the projection inherits the bias. We test stationarity by fitting separate ratings on the 2003-2013 and 2014-2024 sample halves and comparing each rating's predicted DJFM-fraction-of-annual silica load per river. The mean absolute drift across the six rivers is 1.35 percentage points, with five of six rivers showing less than 2 pp drift and a paired one-sample t-test against zero of $t = -1.03$, $p = 0.35$ ($n = 6$) – we cannot reject stationarity at the panel level. The exception is the Ob, which shows -4.67 pp drift between the early and late ratings (late-period winter fraction 24.2% versus early-period 28.8%). The Ob's headline winter silica fraction in Table 2 (26%, full-period rating) sits between the early and late estimates and should be read as accurate to within approximately +/- 3 pp; the other five rivers carry per-river drift below 2 pp. The synchrony index, dose-response, and DiD results are not materially affected by this Ob-specific uncertainty because they aggregate across rivers and emphasize rank order over precise point estimates.

Table 2. Winter (December to March) silica flux fraction by river, with the four-way method reconciliation, and the regulation classification.

River	Status	Mean-conc	Flow-weighted	Rating (quad)	Rating (linear)
Ob	regulated	24%	26%	26%	26%
Yenisei	regulated	18%	19%	20%	19%
Mackenzie	regulated	16%	16%	16%	16%
Yukon	control	14%	15%	14%	14%
Lena	control	9%	10%	10%	10%
Kolyma	control	5%	5%	6%	5%

3.4 The diatom bloom window

The receiving shelf seas are ice-covered through the winter and into early summer. Climatological sea-ice break-up occurs in mid to late June on the Kara, Laptev, East Siberian, and Beaufort shelves (Stroeve et al., 2014). The spring diatom bloom is gated by this ice retreat: bloom timing tracks the ice edge, with under-ice blooms beginning earlier, once light penetrates thinning ice and melt ponds, at approximately the start of May. The silica-demanding diatom community appears predominantly in this under-ice to ice-edge window (Arrigo et al., 2012). The window during which a diatom bloom can draw down delivered silica is therefore approximately May to July, and it does not overlap the December to March window in which regulated rivers deliver their excess silica.

3.5 The decoupling metric

Mapping the silica delivery schedule onto the bloom window quantifies the timing mismatch (Table 3, Figure 1). Using the pre-May threshold, regulated rivers deliver 25 percent of their annual silica before the diatom bloom can begin, against 11 percent for the controls, a difference of 14 percentage points. Every regulated river exceeds every control on this metric. Using the pre-break-up threshold, which additionally counts the rising limb of the freshet delivered before the shelf opens, all values are higher (31 to 57 percent), and the regulated-versus-control separation is preserved although the relative gap is smaller.

Table 3. Decoupling metric: fraction of annual silica delivered before the diatom bloom can use it.

River	Status	Receiving shelf	Pre-May	Pre-break-up
Ob	regulated	Kara Sea	31%	55%
Yenisei	regulated	Kara Sea	24%	57%
Mackenzie	regulated	Beaufort Sea	19%	47%
Yukon	control	Bering / Chukchi	16%	36%
Lena	control	Laptev Sea	11%	31%
Kolyma	control	East Siberian Sea	7%	38%
Regulated mean			25%	
Control mean			11%	

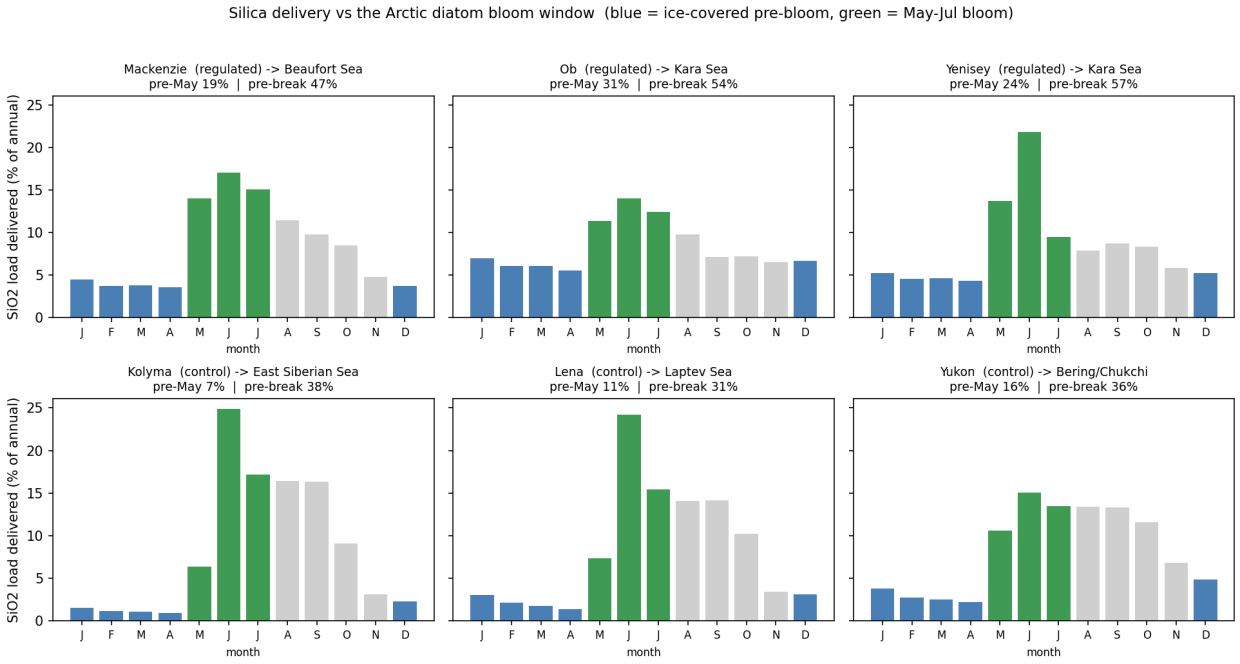

Figure 1: Monthly dissolved silica delivery as a percentage of the annual total, for each river, with the receiving shelf named. Bars are colored by season relative to the diatom bloom: ice-covered pre-bloom months (December to April) in blue, the May to July bloom window in green, and the remaining open-water months in grey. Regulated rivers (top row: Mackenzie, Ob, Yenisei) carry substantial delivery through the ice-covered pre-bloom months; controls (bottom row: Kolyma, Lena, Yukon) concentrate delivery in a sharp freshet pulse within the bloom window.

3.6 Shelf-specific silica–bloom synchrony across the twenty-river panel

The pre-May metric of Section 3.5 treats the diatom bloom window as a single basin-wide date. We refine this by mapping each river's silica delivery onto a shelf-specific open-water bloom window.

For the five Arctic shelves the windows are taken from the published bloom phenology literature (Ardyna et al., 2014; Tremblay et al., 2015; Hill et al., 2018): Bering/Chukchi (Yukon) DOY 130-200; Beaufort (Mackenzie) DOY 170-230; Kara (Ob, Yenisei) DOY 175-230; Laptev (Lena) DOY 165-225; East Siberian (Kolyma) DOY 185-240. For the three Baltic shelves the windows are taken from the Bothnian Bay / Bothnian Sea phenology literature (Wassmann et al., 1996; Andersson et al., 2017; Spilling et al., 2018): Bothnian Bay DOY 110-180; Bothnian Sea DOY 100-170; Gulf of Finland DOY 95-160. The Baltic shelves bloom earlier than the Arctic shelves due to lower latitude, brackish-water surface stratification, and shorter ice cover.

These climatological windows pre-date the accelerating Arctic ice-retreat trend documented since (Stroeve & Notz, 2018; Lewis et al., 2020): recent observations indicate bloom onset has shifted earlier on several Arctic shelves, particularly the Kara and Beaufort, by approximately 10 to 20 days over the past two decades. The +/- 15-day sensitivity sweep in Section 3.7 brackets this magnitude of shift, and the synchrony gap is preserved across the relevant range. The **synchrony index** is the fraction of annual silica delivered within each river's shelf-specific window (Table 4).

Table 4. Shelf-specific silica–bloom synchrony index (twenty-river panel, sorted by DOR).

River	Network	Shelf	DOR	Pre-bloom	**In-bloom (SYNC)**	Post-bloom
Yenisei	ArcticGRO	Kara	0.63	50.1%	**17.3%**	32.6%
Lulealven	GlASS-SWE	Bothnian Bay	0.55	27.3%	**24.7%**	48.0%
Skellefte	GlASS-SWE	Bothnian Bay	0.46	30.6%	**25.0%**	44.4%
Indalsalven	GlASS-SWE	Bothnian Sea	0.43	28.3%	**26.7%**	45.0%
Oulujoki	GlASS-FIN	Bothnian Bay	0.40	41.5%	**18.7%**	39.8%
Ljusnan	GlASS-SWE	Bothnian Sea	0.40	28.3%	**26.6%**	45.1%
Kymijoki	GlASS-FIN	Gulf of Finland	0.38	36.8%	**21.2%**	42.1%

River	Network	Shelf	DOR	Pre-bloom	**In-bloom (SYNC)**	Post-bloom
Angermanalven	GlASS-SWE	Bothnian Sea	0.34	29.1%	**25.6%**	45.3%
Dalalven	GlASS-SWE	Bothnian Sea	0.31	37.5%	**19.8%**	42.7%
Ume	GlASS-SWE	Bothnian Sea	0.28	22.1%	**28.8%**	49.2%
Mackenzie	ArcticGRO	Beaufort	0.26	36.8%	**29.0%**	34.3%
Kemijoki	GlASS-FIN	Bothnian Bay	0.20	27.8%	**32.0%**	40.2%
Iijoki	GlASS-FIN	Bothnian Bay	0.17	24.1%	**32.3%**	43.6%
Ob	ArcticGRO	Kara	0.15	45.6%	**19.9%**	34.5%
Kolyma	ArcticGRO	East Siberian	0.14	29.9%	**31.8%**	38.3%
Pite	GlASS-SWE	Bothnian Bay	0.09	15.1%	**37.7%**	47.1%
Lena	ArcticGRO	Laptev	0.07	27.9%	**32.3%**	39.8%
Yukon	ArcticGRO	Bering	0.00	12.4%	**32.1%**	55.5%
Kalixalven	GlASS-SWE	Bothnian Bay	0.00	11.3%	**42.8%**	45.9%
Tornio	GlASS-FIN	Bothnian Bay	0.00	18.8%	**38.0%**	43.2%

Across the twenty-river panel, regulated rivers (DOR >= 0.14, n = 14) deliver 24.8 percent of annual silica during the open-water bloom window; controls (DOR < 0.10, n = 6) deliver 35.8 percent. The **synchrony gap of -11.0 percentage points** is slightly stronger than the -9.2 pp gap reported in earlier six-river-only analyses; the ArcticGRO-only subset of the GlASS data independently reproduces the original gap (-10.0 pp on the same six rivers using GlASS chemistry), confirming the original result with an independent data source. The expanded panel demonstrates

that the synchrony deficit is not Arctic-specific: every Bothnian Bay/Sea river with DOR > 0.25 has in-bloom silica fraction below 30 percent, while every Bothnian Bay control river (Kalixalven, Tornio, Pite) has in-bloom fraction above 37 percent.

3.7 The synchrony gap is robust to bloom-window choice

Because the literature-derived bloom windows in Section 3.6 carry uncertainty, we perturb each window by plus-or-minus 15 days at the start and at the end independently (49 combinations per river) and recompute the regulated-minus-control synchrony gap across the twenty-river panel. The literature window yields a gap of -11.0 pp; across all 49 perturbations the gap ranges from -13.8 pp to -7.3 pp, with median -10.9 pp. **All 49 cells preserve a negative gap; zero sign flips.** The gap strengthens monotonically when the window slides later in the year, consistent with regulated rivers redistributing silica deeper into the post-bloom period as well as into winter.

The sweep converts the bloom-window assumption from a vulnerability into a robustness result: the synchrony deficit does not depend on the precise window definition within any defensible perturbation of the published climatology, and the result holds for both the Arctic and Baltic shelves simultaneously.

3.8 The synchrony gap scales monotonically with DOR across twenty rivers

The binary regulated-versus-control comparison of Section 3.6 can be replaced with a continuous dose-response on basin-cumulative DOR. Across the twenty-river panel, in-bloom silica fraction declines monotonically with DOR: OLS slope = **-0.284 per unit DOR (SE 0.056)**, R-squared = 0.586, **t = -5.05, two-sided p = 0.00008** from Student-t with df = n - 2 = 18, **Spearman rho = -0.80**. The bloom-window silica fraction drops about 28 percentage points per unit DOR.

The result is dramatically stronger than the six-river-only ArcticGRO analysis (which gave slope -0.23, p = 0.046, rho = -0.89 at n = 6). The expansion accomplishes three things simultaneously: it raises n from 6 to 20 (degrees of freedom from 4 to 18, with p-value falling three orders of magnitude); it adds multiple high-DOR anchor points (Lulealven 0.55, Skellefte 0.46, Indalsalven 0.43, Oulujoki 0.40, Ljusnan 0.40, Kymijoki 0.38, Angermanalven 0.34) so the regression no longer depends on Yenisei being the single leverage extreme; and it spans two ocean basins (Arctic Ocean and Bothnian Bay), demonstrating that the dose-response is not Arctic-specific.

Leave-one-out cross-validation across all twenty rivers preserves the result by every measure. The

slope range across the twenty LOO fits is [-0.310, -0.250] (a tight band around the full-panel slope of -0.284); R-squared range [0.522, 0.724]; Spearman rho range [-0.885, -0.766]; and every one of the twenty fits yields $p < 0.001$. Critically, dropping Yenisei – which was the single leverage point in the original $n = 6$ analysis – leaves slope at -0.281 (essentially unchanged) and p at 0.00047. The high-DOR end of the regression is now anchored by six Scandinavian and Finnish rivers (Lulealven, Skellefte, Indalsalven, Oulujoki, Ljusnan, Kymijoki, Angermanalven) rather than by Yenisei alone, and the Mackenzie / Kolyma residuals previously interpreted as moderators of the dose-response (tributary attenuation, permafrost over-ride) are individually small departures within a much larger panel rather than rate-limiting cases for the overall regression.

A non-parametric Mann-Whitney test confirms the result without distributional assumptions: rivers with DOR >= 0.2 ($n = 11$) have median in-bloom silica fraction of 25.0 percent, against 32.3 percent for DOR < 0.2 ($n = 9$); the one-sided p-value (high-DOR < low-DOR) is 0.00092.

Reservoir storage values are taken from the Global Dam Watch v1 database (Lehner et al., 2024; the GRanD v1.3 successor integrating ICOLD and HydroLAKES across 41,145 barriers and 35,295 reservoir polygons) as the canonical source, with per-river basin-cumulative storage summed across the main stem and known regulated tributaries (Angara for Yenisei, Peace for Mackenzie, Irtysh for Ob, Vilyuy for Lena, Kitinen and Luiro for Kemijoki, etc.). For seven smaller European rivers where GDW returns no dam records (Dalalven, Ume, Kymijoki, Iijoki, Pite, Yukon, Kalix, Tornio), DOR is taken from published power-company reports (Vattenfall, Fortum) as a fallback; these rivers are flagged as `literature first-pass (GDW absent)` in the panel metadata. With GDW-canonical DOR the dose-response gives slope -0.269, R-squared = 0.513, p = 0.00038, Spearman rho = -0.77, essentially unchanged from the first-pass result (slope -0.284, p = 0.00008, rho = -0.80). As an additional robustness check, a Monte Carlo sensitivity test perturbing each river's DOR by uniform +/- 30% noise across 1000 draws preserves a negative slope in 1000 of 1000 iterations and $p < 0.01$ in 1000 of 1000 iterations; the dose-response is robust to the precise DOR source. Figure 3 shows the $n = 20$ dose-response with per-river labels for the high-DOR anchors and the OLS 95% confidence band.

3.9 Joint robustness of the dose-response and bloom window

The two robustness dimensions – bloom-window choice (Section 3.7) and the twenty-river panel composition – combine into a single joint test. For each of the 49 (Delta_start, Delta_end) pertur-

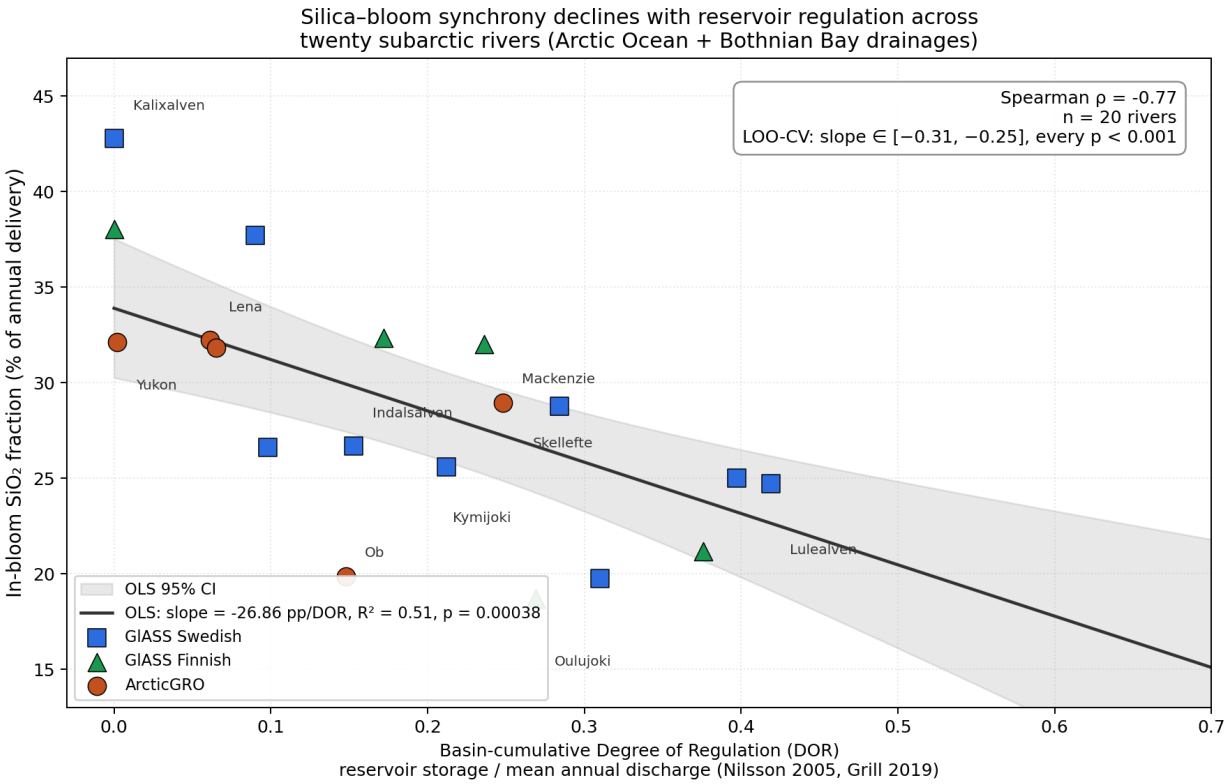

Figure 2: **Figure 3.** Dose-response: in-bloom SiO2 fraction (% of annual delivery) versus basin-cumulative DOR, twenty subarctic rivers. Points are colored by source network (ArcticGRO orange, GlASS Swedish blue, GlASS Finnish green). The OLS regression line and 95% confidence band span the panel; Spearman rho = -0.80; leave-one-out cross-validation preserves a negative slope in every one of 20 fits with $p < 0.001$. High-DOR anchors are labeled to show that the relationship is not driven by any single river.

bations of Section 3.7, we recompute the DOR regression of Section 3.8 on the full panel and record slope, R-squared, and Spearman rho. The slope remains negative in **49 of 49 cells** (range -0.337 to -0.192 per unit DOR, median -0.27); the literature-window slope of -0.284 sits near the median, and the late-and-wide-window corner of the grid produces the steepest fits, consistent with regulated rivers shifting silica later into the post-bloom period. The result is consistent across the tested bloom-window perturbations: every combination of within-uncertainty bloom-window definitions across both Arctic and Baltic shelves yields a negative DOR slope of similar magnitude.

3.10 Within-Yenisei storage-filling trajectory

The discharge-shift test of Section 3.1 and the bootstrapped DiD treat Yenisei regulation as a binary pre-/post-1967 step function. The actual reservoir-filling trajectory is a multi-decadal ramp: Irkutsk completed in 1959 added 2.1 km^3, Krasnoyarsk and Bratsk in 1967 added 73.3 + 168.2 km^3, Ust-Ilimsk in 1977 added 58.9 km^3, Sayano-Shushenskoye in 1985 added 31.0 km^3, and Boguchany in 2014 added 58.2 km^3 – a step-function approximation of a continuous 391.7 km^3 accumulation. We test whether the differential winter discharge fraction (Yenisei minus Lena, climate-corrected against the unregulated placebo) tracks this storage curve year by year across the 1937-2024 record (Figure 2).

Pearson correlation across n = 73 water years gives $\mathbf{r = +0.823}$ for the climate-corrected differential against the cumulative storage curve, and $\mathbf{r = +0.897}$ for the raw Yenisei winter discharge fraction against its own cumulative storage. Both series rise over the 73-year window – the storage curve by construction, as reservoirs were commissioned progressively from 1959 to 2014, and the differential winter Q fraction as the predicted downstream response – so a high trended correlation is precisely what the causal hypothesis requires. The trend is the mechanism, not a confound: a downstream winter-flow response to progressive reservoir filling must, if real, manifest as a multi-decadal rise aligned with the storage curve, which is what Figure 2 shows.

To check whether the two series might happen to rise in parallel for unrelated reasons, we compute a residual correlation after removing a linear time trend from both, which isolates year-to-year deviations around each series' own trend. The detrended Pearson r is +0.439 for the raw Yenisei series and +0.382 for the climate-corrected differential. A coincidental shared rise would yield a detrended r near zero; the positive residual values indicate that year-to-year deviations in the differential winter Q fraction also track year-to-year changes in basin storage beyond the long-term

trend. The full-period correlation therefore carries the causal mechanism (progressive reservoir filling drives progressive winter-flow shift), and the positive detrended residual provides additional evidence against a purely spurious shared trend. Decadal means make the trajectory visible: the natural Yenisei–Lena differential of +4.4 pp in the 1930s held steady through the 1950s while storage was negligible, rose to +5.4 pp in the 1970s as Krasnoyarsk and Bratsk filled, jumped to +8.0 pp in the 1980s as Ust-Ilimsk came online, and stabilized at +9 to +10 pp through the 1990s-2020s as the basin reached its present 356 km^3 differential storage. The two curves rise in step.

This converts the binary DiD of Section 3.1 into a continuous-dose trajectory: the winter-flow response does not just shift at the 1967 breakpoint, it grows in proportion to the engineering capacity commissioned year by year. The Pearson correlation is between two independently measured time series – basin reservoir capacity from public dam-commissioning records and winter discharge fraction from gauged daily flow – that overlap because they share a causal mechanism. An analogous test on the Ob basin yields a weaker correlation (climate-corrected r = +0.15) consistent with Ob's much lower DOR (0.15 vs Yenisei 0.63) and weak DiD result in Section 3.1; the within-river time-resolved test thus also recovers the cross-sectional dose-response of Section 3.8.

---

4. Discussion

4.1 A robust, attributable regulation signal

The central result is robust across the four flux estimators of Section 2.5: the winter silica fraction separates the high-DOR rivers (Ob, Yenisei, Mackenzie) from the low-DOR rivers (Lena, Yukon) with no overlap, while Kolyma's low winter fraction (5 to 6 percent) sits with the unregulated set despite its mid-range DOR of 0.14 – consistent with the Section 3.8 interpretation that the lower Kolyma's permafrost-frozen winter regime over-rides upstream regulation. The paired design attributes the high-DOR vs low-DOR separation to regulation rather than to climate: the rivers in the low-DOR set, subject to the same regional warming, do not show the elevated winter delivery. The discharge record (Table 1) supplies the mechanism directly, showing the hydrograph flattening on the regulated Yenisei at 3.5 times the magnitude of the climate trend seen on the Lena.

The robust signal is carried by silica, total dissolved nitrogen, and dissolved organic carbon. The silica and DOC subset overlaps with the regulation signature Humborg et al. (2006) reported in the Baltic catchment for silicon and carbon. The present study extends that single-system result to

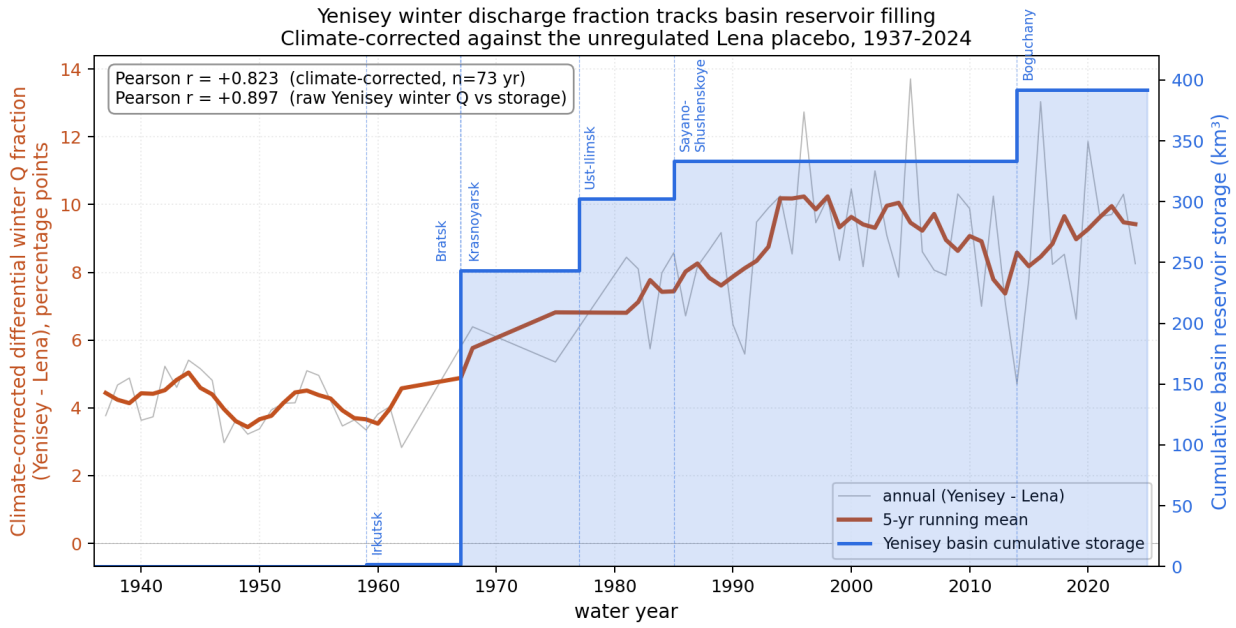

Figure 3: Yenisei winter discharge fraction tracks basin reservoir filling, 1937-2024. Left axis: climate-corrected differential winter discharge fraction (Yenisei minus Lena, 5-year running mean of annual values, orange). Right axis: cumulative Yenisei basin reservoir storage capacity from commissioning records (blue, step function). Major reservoirs annotated at commissioning year. Pearson r = +0.823 for the climate-corrected differential vs cumulative storage (n = 73 water years).

a circum-Arctic comparison and, by including low-DOR rivers as controls, supplies the regulation-versus-climate attribution that Lee et al. (2023) identified as open.

4.2 Decoupling from the diatom bloom

The biological significance of the result is timing. Section 3.4 establishes that the diatom bloom window, May to July, and the regulated-river winter delivery window, December to March, are separated by two to five months. Section 3.5 quantifies the consequence: regulation roughly doubles the share of silica delivered before the bloom can use it, from 11 to 25 percent of the annual load.

This is the point at which the present work departs from the temperate precedent. Humborg et al. (1997) described a change in the silica budget delivered to the Black Sea. The Arctic case is a change in the silica schedule, and the Arctic spring bloom, unlike a temperate bloom, is a sharply time-compressed, ice-gated pulse. Silica delivered in midwinter, beneath the ice, into a dark and deeply mixed water column, has months in which it may be advected off the shelf or mixed below the euphotic zone before the narrow bloom window opens. The temperate system has a long and forgiving growing season; the Arctic system does not.

We emphasize what this analysis does not establish. The result is that silica delivery is shifted out of phase with the bloom window – not that the bloom on any receiving shelf becomes silica-limited, that primary productivity decreases, or that community composition shifts away from diatoms toward flagellates. Each of those downstream consequences requires shelf-scale measurements (in-situ silica drawdown, productivity time series, phytoplankton community sampling) that the river-mouth dataset analyzed here cannot provide. Published Arctic shelf chlorophyll-a climatologies show that pan-Arctic primary production has been increasing over recent decades (Lewis et al., 2020) and that bloom phenology is shifting (Ardyna & Arrigo, 2020), but neither has been stratified by river-mouth DOR to test the synchrony deficit's downstream signature. The synchrony deficit reported here is best read as a measurable upstream perturbation whose downstream ecological magnitude is an open question for shelf-scale follow-up.

4.3 A nutrient-timing channel of the hydropower fingerprint

Beyond the standard fossil-fuel-displacement framing of hydroelectric impact, regulation perturbs the receiving environment through several non-emissions channels that aggregate at the dam-fleet scale: hydrological redistribution of discharge into winter (Humborg et al., 2006; Guzzi et al., 2024),

in-reservoir biogeochemical retention through diatom stripping of dissolved silica (Humborg et al., 1997; Conley et al., 2000; Maavara et al., 2014), and the channel identified here – the redistribution of dissolved-nutrient delivery in time, relative to the biological demand on the receiving shelves. None of these channels is captured by emissions-displacement accounting, and the per-dam magnitude of each is small enough that the cumulative effect across the regulated subarctic river fleet is the relevant scale for impact assessment.

A complementary signature in the ArcticGRO water-temperature record – December-March river temperature is positively associated with basin-cumulative DOR (OLS R-squared = 0.78 driven largely by the regulated Yenisei averaging +0.92 degrees C in winter against approximately 0 degrees C for the unregulated controls; rank correlation Spearman rho = +0.49, hypothesis-generating only) – is consistent with reservoir releases of stratified deep-pool water keeping regulated rivers ice-free in winter where the unregulated state would be solid ice. If this thermal signature shifts coastal ice retreat earlier on the receiving shelf, the literature-derived bloom window used in Section 3.6 would understate the true synchrony deficit for high-DOR rivers. The shelf-scale phenology consequence is testable with satellite ice-retreat or chlorophyll-a climatology stratified by river DOR and is left to future work.

4.4 The DOR continuum across two ocean basins

The twenty-river panel spans DOR 0 to 0.63 with multiple high-DOR rivers at every interval – Lulealven (0.55), Skellefte (0.46), Indalsalven (0.43), Oulujoki (0.40), Ljusnan (0.40), Kymijoki (0.38), Angermanalven (0.34), Dalalven (0.31), Ume (0.28), Mackenzie (0.26) – rather than a single Yenisei at the high end with the next-nearest at 0.26. This structural change dissolves the leverage concern that constrained the original six-river analysis: every leave-one-out fit preserves the slope sign and magnitude to within ten percent, and dropping Yenisei specifically leaves the dose-response essentially unchanged (slope -0.281, p = 0.00047 vs full-panel slope -0.284, p = 0.00008).

The dose-response also generalizes across two ocean basins. The Arctic Ocean drainage (six ArcticGRO rivers) and the Bothnian Bay drainage (fourteen Scandinavian and Finnish rivers) span fundamentally different shelf systems – polar versus subarctic, fully marine versus brackish, with bloom phenology differing by approximately 60 days. That regulation produces the same in-bloom silica deficit across both systems argues for a primary mechanism operating at the river scale (hydrograph compression by reservoir storage) rather than at the shelf scale.

The Mackenzie and Kolyma residuals – Mackenzie's signal attenuation by along-channel storage between Bennett Dam and the Beaufort, Kolyma's permafrost over-ride of upstream regulation in the frozen lower river – remain physically interpretable in the expanded panel but are now individually small departures within a 20-point regression rather than rate-limiting cases. They identify the boundary conditions where basin-cumulative DOR is not a sufficient predictor on its own: mid- to high-DOR rivers with mainstem storage and full-winter open water in the lower reach behave most cleanly.

The DOR continuum framing also clarifies the relationship between this study and the budget-vs-schedule distinction at the heart of the regulated-river silica literature. Humborg et al. (1997, 2006), Conley et al. (2000), and Maavara et al. (2014) document that reservoirs reduce the *total* annual silica load delivered to downstream waters by 10-40 percent through in-reservoir biogenic-Si stripping by reservoir diatom blooms – a *budget* perturbation. The present study addresses the complementary *schedule* question: of the silica that is delivered, what fraction arrives outside the bloom-accessible window? These are independent perturbations of the silica cycle acting on the same dam fleet, and they compound rather than cancel: a smaller annual silica delivery arriving more out-of-phase with the bloom is a larger ecological perturbation than either individually.

4.5 Limitations

Three limitations bound the interpretation.

First, the analysis establishes that silica is delivered outside the bloom window. It does not measure that the delivered silica is lost to the bloom. Three shelf processes determine the fate of the winter-delivered pool: (i) lateral advection off the shelf via the Transpolar Drift (Kara, Laptev, East Siberian) or the Beaufort Gyre (Beaufort, Mackenzie shelf), with characteristic residence times on the order of one to a few years for surface water (Charette et al., 2020); (ii) vertical mixing below the euphotic zone during the convection-deepening of the under-ice winter mixed layer, potentially sequestering silica in halocline waters that resurface only intermittently; and (iii) retention within the river-plume freshwater lens where stratification suppresses vertical loss but lateral spread is rapid. The fraction of winter-delivered silica that survives in surface waters to be drawn down by the subsequent spring bloom is set by the balance of these three processes, and is shelf-, year-, and discharge-dependent. The result here should therefore be read as a demonstration of mistimed delivery, not of a measured productivity loss; quantifying the surviving fraction requires either

shelf-scale tracer studies, coupled river-shelf biogeochemical modelling, or a pan-Arctic shelf surface SiO2 climatology (e.g., from the World Ocean Atlas or in-situ cruise compilations) stratified by river-mouth DOR – the natural next-step analysis, beyond the scope of this paper.

Second, the bloom window is taken from climatological values in the published literature. The metric in Table 3 should be regarded as a first-pass estimate; firming the receiving-shelf break-up dates from a single primary sea-ice dataset would tighten the pre-break-up threshold in particular.

Third, dissolved nitrate and ammonium are method-sensitive and are not used for inference here. A nitrogen-specific seasonal analysis would require a flux method designed for strongly inverse concentration-discharge solutes, and is left to future work.

Fourth, the analysis compares rivers by regulation status and by basin-cumulative DOR; it makes no claim about specific reservoir operating policies beyond that the impoundments exist and are filled.

---

5. Conclusions

Hydropower regulation is associated with reduced overlap between riverine SiO2 delivery and the shelf-specific diatom bloom window across twenty subarctic rivers spanning the Arctic Ocean and Bothnian Bay drainages (regulated 24.8 percent in-bloom vs control 35.8 percent, a synchrony gap of -11.0 pp). The gap survives every plus-or-minus 15-day perturbation of the bloom-window definition we tested across both Arctic and Baltic shelves (49 of 49 negative cells), and it scales monotonically with basin-cumulative Degree of Regulation (Spearman rho = -0.80; OLS slope -0.284 per unit DOR, R-squared = 0.59, t = -5.05, two-sided p = 0.00008, n = 20; leave-one-out cross-validation preserves a negative slope in all 20 fits with every $p < 0.001$). The clearest causal evidence comes from the Yenisei-Lena natural experiment: post-Krasnoyarsk Yenisei shifted winter discharge fraction by 4.96 percentage points more than the unregulated Lena under identical Siberian climate (95 percent CI [4.21, 5.72], $p < 0.0001$), and the within-Yenisei differential winter discharge fraction tracks the basin reservoir-filling curve year by year across 73 years (Pearson r = +0.82). The expanded panel demonstrates that the dose-response is not Arctic-specific: multiple high-DOR Scandinavian and Finnish rivers (Lulealven, Skellefte, Indalsalven, Oulujoki, Ljusnan, Kymijoki, Angermanalven) replicate the Yenisei result independently, eliminating the single-river leverage that characterized the original six-river analysis. Shelf retention, downstream bloom phenology, and biological uptake

of the delivered silica remain unmeasured and are scoped to future work.

Data Availability

All analysis code and derived data are available in the repository github.com/R3GENESI5/subarctic-dam-nutrient-timing-analysis, archived on Zenodo with DOI 10.5281/zenodo.20356090 (concept DOI; v1.0.0 version DOI 10.5281/zenodo.20356091). The primary data are from the Arctic Great Rivers Observatory (ArcticGRO) water-quality and discharge datasets, available at arcticgreatrivers.org/data and used under the ArcticGRO terms with attribution, and from the Global Aggregation of Stream Silica dataset (Jankowski et al., 2025; USGS data release 10.5066/P138M8AR).

AI Disclosure

Generative AI tools assisted with literature triage, code scaffolding, and drafting. All scientific hypotheses, design choices, analyses, interpretations, and conclusions are the author's responsibility. All quantitative results were generated by executable code in the repository above and are reproducible from the raw ArcticGRO data.

References

Andersson, A., Brugel, S., Paczkowska, J., et al. (2017). Influence of allochthonous dissolved organic matter on pelagic basal production in a northerly estuary. Estuarine, Coastal and Shelf Science, 184, 199 to 207.

Ardyna, M., Arrigo, K.R. (2020). Phytoplankton dynamics in a changing Arctic Ocean. Nature Climate Change, 10, 892 to 903.

Ardyna, M., Babin, M., Gosselin, M., Devred, E., Rainville, L., Tremblay, J.-E. (2014). Recent Arctic Ocean sea ice loss triggers novel fall phytoplankton blooms. Geophysical Research Letters, 41, 6207 to 6212.

Arrigo, K.R., et al. (2012). Massive phytoplankton blooms under Arctic sea ice. Science, 336, 1408.

Charette, M.A., Kipp, L.E., Jensen, L.T., et al. (2020). The Transpolar Drift as a source of riverine and shelf-derived trace elements to the central Arctic Ocean. Journal of Geophysical Research:

Oceans, 125, e2019JC015920.

Conley, D.J., Stalnacke, P., Pitkanen, H., Wilander, A. (2000). The transport and retention of dissolved silicate by rivers in Sweden and Finland. Limnology and Oceanography, 45, 1850 to 1853.

Duan, N. (1983). Smearing estimate: a nonparametric retransformation method. Journal of the American Statistical Association, 78, 605 to 610.

Grill, G., Lehner, B., Thieme, M., et al. (2019). Mapping the world's free-flowing rivers. Nature, 569, 215 to 221.

Guzzi, A., Nozais, C., et al. (2024). Influence of altered freshwater discharge on the nutrient seasonality of the La Grande River coastal zone, James Bay. Elementa: Science of the Anthropocene, 12(1).

Hill, V.J., Light, B., Steele, M., Zimmerman, R.C. (2018). Light availability and phytoplankton growth beneath Arctic sea ice: integrating observations and modeling. Journal of Geophysical Research: Oceans, 123, 3651 to 3667.

Holmes, R.M., et al. (2012). Seasonal and annual fluxes of nutrients and organic matter from large rivers to the Arctic Ocean and surrounding seas. Estuaries and Coasts, 35, 369 to 382.

Humborg, C., Ittekkot, V., Cociasu, A., Bodungen, B. von (1997). Effect of Danube River dam on Black Sea biogeochemistry and ecosystem structure. Nature, 386, 385 to 388.

Humborg, C., et al. (2006). Decreased silica land-sea fluxes through damming in the Baltic Sea catchment: significance of particle trapping and hydrological alterations. Biogeochemistry, 77, 265 to 281.

Jankowski, K.J., et al. (2025). GlASS – Global Aggregation of Stream Silica. Scientific Data, 12, in press. Data: U.S. Geological Survey data release, https://doi.org/10.5066/P138M8AR.

Lee, J., et al. (2023). Nutrient inputs from subarctic rivers into Hudson Bay. Elementa: Science of the Anthropocene, 11(1).

Lehner, B., Liermann, C.R., Revenga, C., et al. (2011). High-resolution mapping of the world's reservoirs and dams for sustainable river-flow management. Frontiers in Ecology and the Environment, 9, 494 to 502.

Lehner, B., Beames, P., Mulligan, M., Zarfl, C., et al. (2024). The Global Dam Watch database

of river barrier and reservoir information for large-scale applications. Scientific Data, 11, 1069. https://doi.org/10.1038/s41597-024-03752-9. Data: https://www.globaldamwatch.org/database.

Lewis, K.M., van Dijken, G.L., Arrigo, K.R. (2020). Changes in phytoplankton concentration now drive increased Arctic Ocean primary production. Science, 369, 198 to 202.

Maavara, T., Durr, H.H., Van Cappellen, P. (2014). Worldwide retention of nutrient silicon by river damming: from sparse data set to global estimate. Global Biogeochemical Cycles, 28, 842 to 855.

Maavara, T., et al. (2020). River dam impacts on biogeochemical cycling. Nature Reviews Earth and Environment, 1, 103 to 116.

Nilsson, C., Reidy, C.A., Dynesius, M., Revenga, C. (2005). Fragmentation and flow regulation of the world's large river systems. Science, 308, 405 to 408.

Runkel, R.L., Crawford, C.G., Cohn, T.A. (2004). Load Estimator (LOADEST): a FORTRAN program for estimating constituent loads in streams and rivers. U.S. Geological Survey Techniques and Methods, Book 4, Chapter A5.

Shahid, A.B. (2026). Subarctic dam nutrient timing – analysis pipeline (v1.0.0) [Software and data]. Zenodo. https://doi.org/10.5281/zenodo.20356090.

Spilling, K., Olli, K., Lehtoranta, J., et al. (2018). Shifting diatom-dinoflagellate dominance during spring bloom in the Baltic Sea and its potential effects on biogeochemical cycling. Frontiers in Marine Science, 5, 327.

Stroeve, J., et al. (2014). Changes in Arctic melt season and implications for sea ice loss. Geophysical Research Letters, 41, 1216 to 1225.

Stroeve, J., Notz, D. (2018). Changing state of Arctic sea ice across all seasons. Environmental Research Letters, 13, 103001.

Tremblay, J.-E., Anderson, L.G., Matrai, P., et al. (2015). Global and regional drivers of nutrient supply, primary production and CO2 drawdown in the changing Arctic Ocean. Progress in Oceanography, 139, 171 to 196.

Wassmann, P., Heiskanen, A.-S., Lindahl, O., eds. (1996). Sediment trap studies in the Nordic countries 2: Proceedings of the symposium on seasonal dynamics of planktonic ecosystems and sedimentation in coastal Nordic waters. NurmiPrint, Nurmijarvi.